Electronic Supplementary Material (ESI) for Journal of Materials Chemistry B.

A Lipid Droplets Specific Fluorescent Probe for Image-Guided Photodynamic Therapy under Hypoxia

Weihua Zhuang[†],[a, b] Ping Tan[†],[c] Shufen Li,[a] Chengming Li,[a] Jiapeng Zhang,[c] Jianzhong Ai,[c] Lu Yang,[c] Gaocan Li,[b] Qiang Wei,[*c] Mao Chen[*a, d], and Yunbing Wang[b]

[a] Laboratory of Heart Valve Disease, West China Hospital, Sichuan University, 37 Guoxue Road, Chengdu 610041, PR China. E-mail: hmaochen@vip.sina.com

[b] National Engineering Research Center for Biomaterials, Sichuan University, 29 Wangjiang Road, Chengdu 610064, PR China.

[c] Department of Urology, Institute of Urology, Huaxi MR Research Center (HMRRC), State Key Laboratory of Biotherapy and Cancer Center, West China Hospital, Sichuan University, 37 Guoxue Road, Chengdu 610041, PR China. E-mail: weiqiang@scu.edu.cn.

[d] Department of Cardiology, West China Hospital, Sichuan University, 37 Guoxue Road, Chengdu 610041, PR China.

[†]These authors contributed equally to this work.

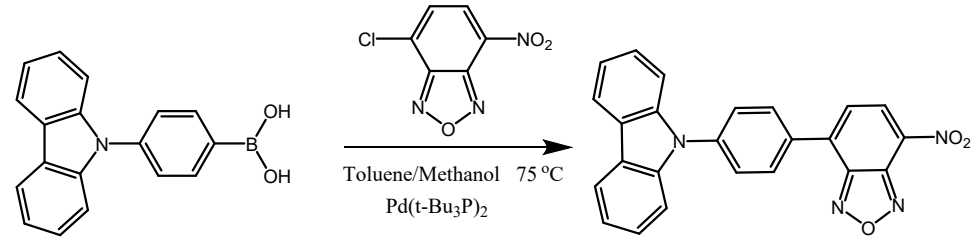

Fig. S1. Synthetic route of **CPNBD**.

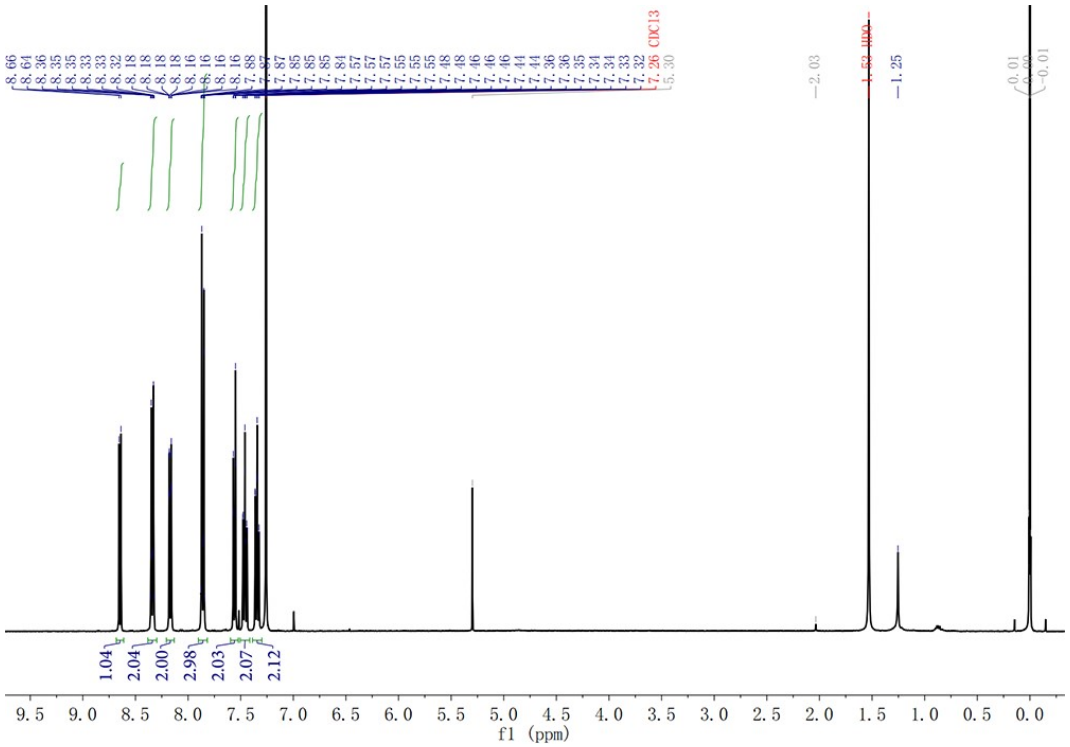

Fig. S2. ^{1}H NMR spectrum of **CPNBD** in $CDCl_3$.

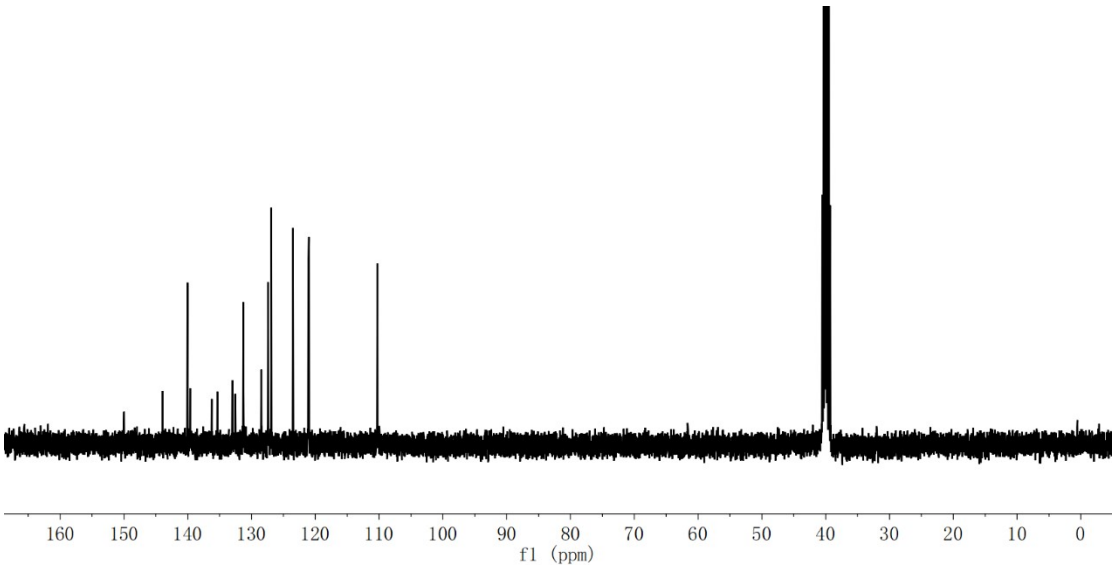

Fig. S3. ^{13}C NMR spectrum of **CPNBD** in DMSO-d_6.

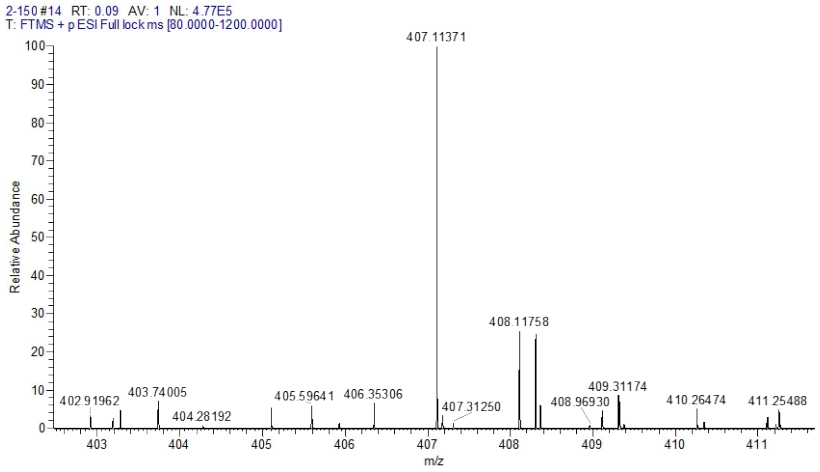

Fig. S4. HR-MS of **CPNBD**.

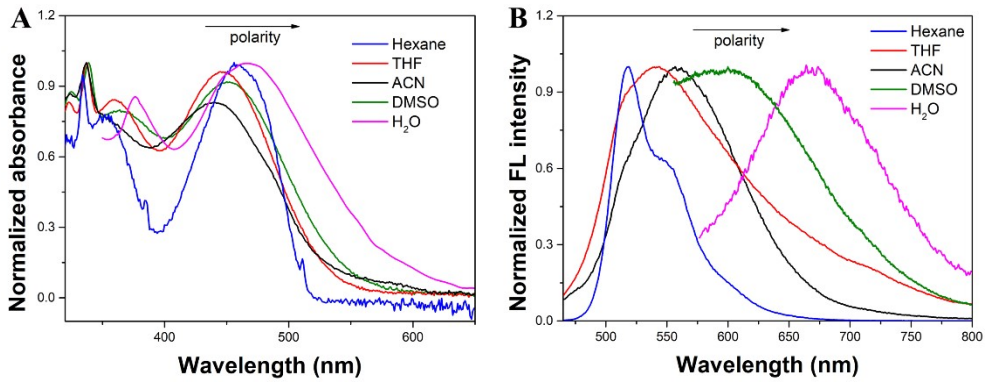

Fig. S5. Normalized UV-vis absorption spectra (A) and normalized FL spectra (B) of **CPNBD** in different solvents with various polarity. **CPNBD** exhibited very low fluorescence emission in DMSO, which was near the raman peaks and it was hard to normalize. Thus, the raman peaks were not shown in (B).

Table S1 photophysical properties of CPNBD.

probe	λ_{abs}/nm ($\varepsilon/10^3$ M^{-1} cm^{-1})	$\lambda_{em\ max}$/nm (H_2O)	$\lambda_{ex\ max}$/nm (oil)	Φ_f(%)			ΦΔ
				H_2O	oil	solid	
CPNBD	9.51735	470	605	≈ 0	15.83	1.17	0.135

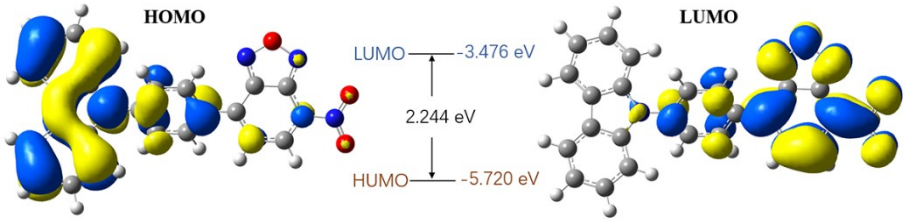

Fig. S6. DFT simulation of HOMO and LUMO energy levels of **CPNBD** (in toluene).

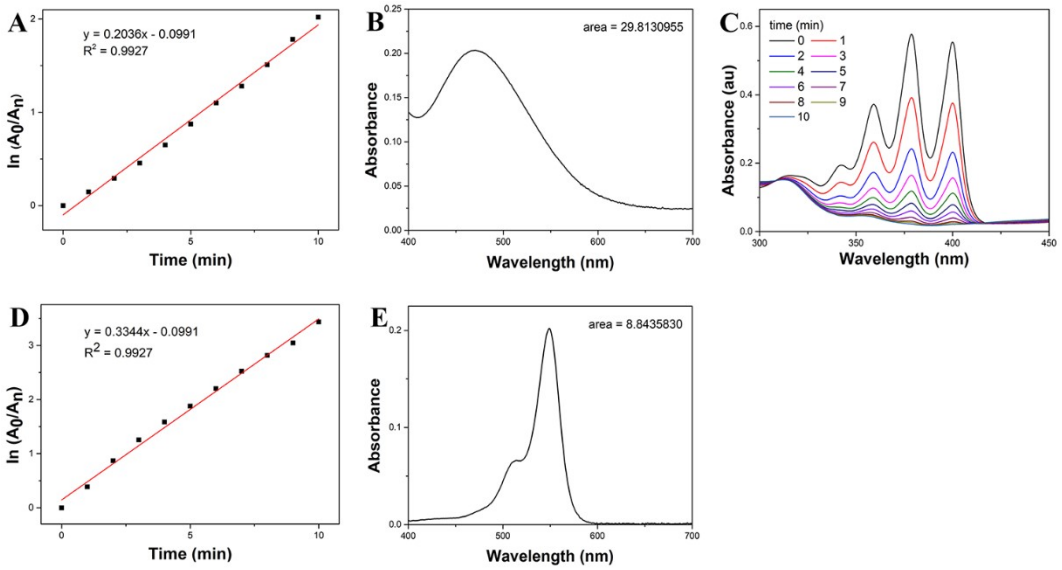

Fig. S7. The absorbance decay of the ABDA at 378 nm under white light irradiation (10 mW.cm^{-2}) in the presence of **CPNBD** (A). The absorption spectrum of CPNBD ranged in 400-700 nm (B). The absorbance decay of the ABDA at 378 nm under white light irradiation (10 mW.cm^{-2}) in the presence of Rose Bengal (C). The absorbance decay of the ABDA at 378 nm under white light irradiation (10 mW.cm^{-2}) in the presence of Rose Bengal (D). The absorption spectrum of Rose Bengal ranged in 400–700 nm (E).

Table S2 Theoretically calculated energy level and energy gap of **CPNBD** (B3LYP/6-31G* level).

S_n	Energy (eV)	T_n	Energy (eV)	S_1/T_n	S_1/T_n Energy gap
S_1	1.96	T_1	1.64	S_1/T_1	0.32
S_2	2.27	T_2	2.11	S_1/T_2	-0.15
S_3	3.22	T_3	2.26	S_1/T_3	-0.64
S_4	3.31	T_4	2.65	S_1/T_4	-0.69
S_5	3.37	T_5	2.95	S_1/T_5	-0.99
S_6	3.48	T_6	3.16	S_1/T_6	-1.20
S_7	3.64	T_7	3.27	S_1/T_7	-1.31
S_8	3.87	T_8	3.30	S_1/T_8	-1.34

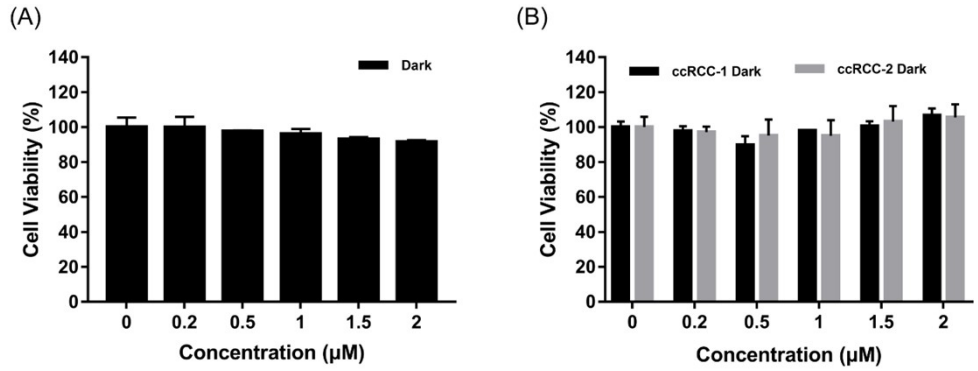

Fig. S8. Cell viability of (A) 786-O cells and (B) human primary ccRCC tumor cells incubated with different concentrations of **CNPBD** for 24 h.

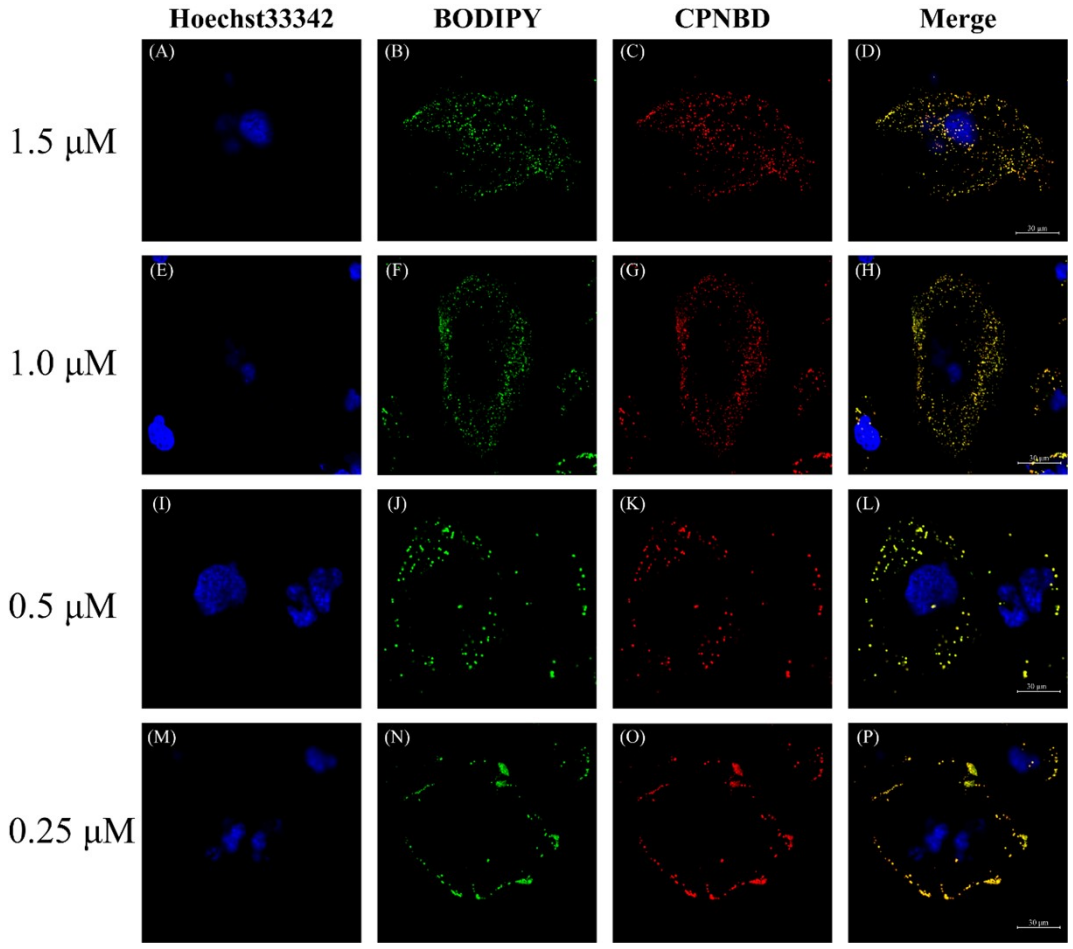

Fig. S9. Colocalization imaging of 786-O cells stained with Hoechst 33342 (λ_{ex} = 405 nm), BODIPY 493/503 (λ_{ex} = 488 nm, 100 nM) and different concentrations of **CPNBD** (λ_{ex} = 488 nm) (A-D) 1.5 μM, (E-H) 1.0 μM, (I-L) 0.5 μM, and (M-P) 0.25 μM. Scale bar, 30 μm. λ_{ex} = 488 nm. Pearson's coefficients (R_r) of Figure S2D, S2H, S2L and S2P were calculated as 99.54%, 99.57%, 99.82% and 99.49%, respectively. Manders' coefficients (m_1 and m_2) of Figure S2D, S2H, S2L and S2P were calculated as 0.99 and 0.97, 0.99 and 0.97, 0.99 and 0.99, 0.99 and 0.97, respectively.

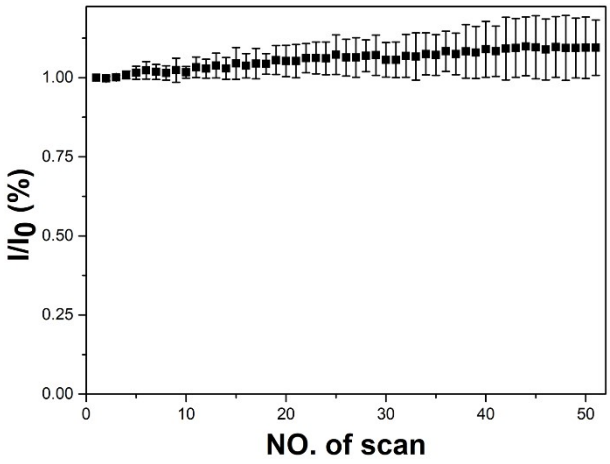

Fig. S10. Remaining emission intensity (I/I_0) of **CPNBD** (2 μM) in 786-O cells with the increasing irradiation time (scanning time: 6.1 s per scan). λ_{ex} = 488 nm.

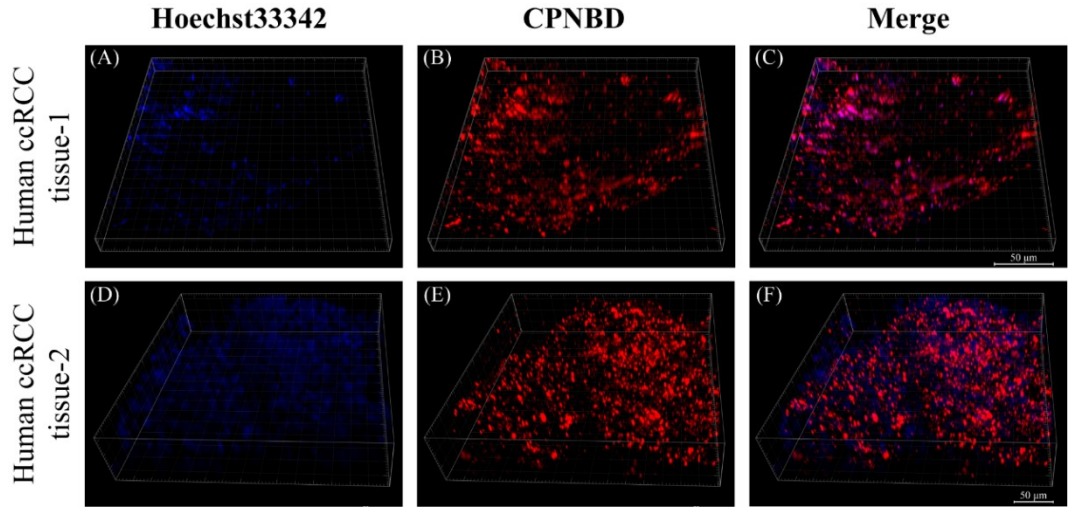

Fig. S11. Representative images of human ccRCC tumor tissues stained with Hoechst 33342 (λ_{ex} = 405 nm, λ_{em} = 500-550 nm) and **CPNBD** (λ_{ex} = 488 nm, λ_{em} = 570-620 nm) in (A-C) patient 1 and (D-F) patient 2. Scale bar, 50 μm.

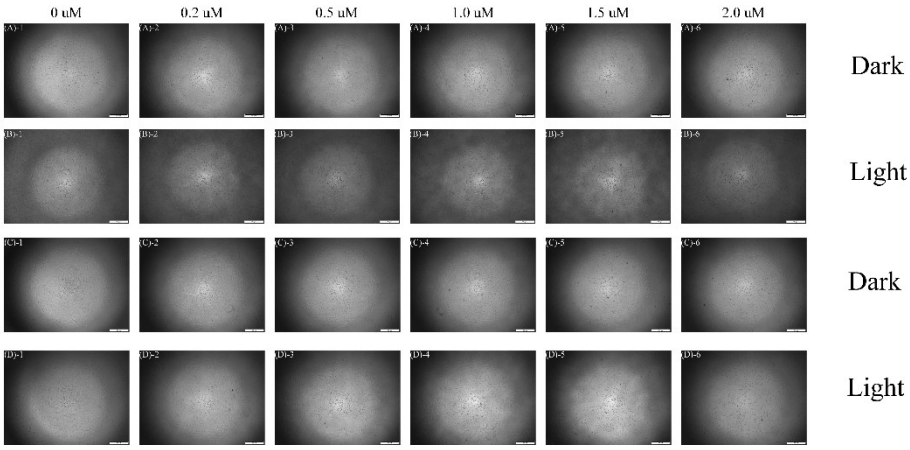

Fig. S12. Cytotoxicity of human primary ccRCC tumor cells from (A-1 to B-6) patient 1 and (C-1 to D-6) patient 2 incubated by different concentrations of **CPNBD** (B1-6, D1-6) with or (A1-6, C1-6) without white radiation for 30 min. Scale bar, 500 μm.

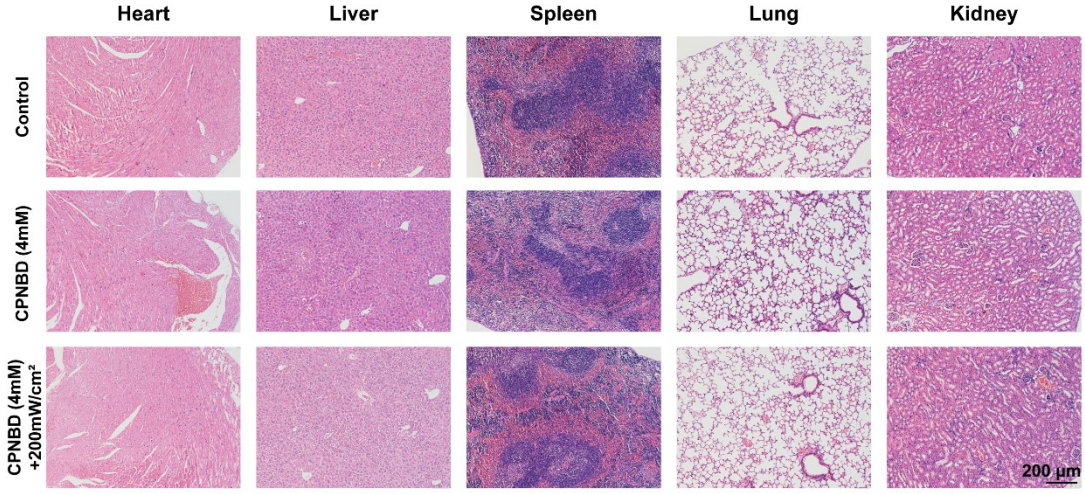

Fig. S13. Representative images of H&E stained main organs from mice after different treatments. Scale bar, 200 μm.